

The structure of focused, radially polarized fields

D. W. Diehl

ASE Optics, Inc.,

2489 Brighton-Henrietta Townline Rd., Rochester, NY 14623, USA

R. W. Schoonover and T. D. Visser

Dept. of Physics and Astronomy, Free University,

De Boelelaan 1081, 1081 HV Amsterdam, The Netherlands

twisser@nat.vu.nl

Abstract: We present a detailed analysis of the structure of strongly focused, radially polarized electromagnetic fields. The existence of phase singularities of the two components of the electric field is demonstrated. Two different mechanisms to obtain creation or annihilation of these phase singularities are discussed. These are changing the aperture angle of the lens and the width of the beam. Also, it is shown that in the focal plane the handedness of the electric polarization ellipse is an alternating function of the radial distance. Finally, the different contributions to the electric energy density are examined.

© 2006 Optical Society of America

OCIS codes: (050.1960) Diffraction theory; (140.3300) Laser beam shaping; (260.2110) Electromagnetic theory; (260.5430) Polarization

References and links

1. K.S. Youngworth and T.G. Brown, "Inhomogeneous polarization in scanning optical microscopy," *Proceedings of SPIE* **3919**, 75–85 (2000).
2. K.S. Youngworth and T.G. Brown, "Focusing of high numerical aperture cylindrical-vector beams," *Opt. Express* **7**, 77–87 (2000),
<http://www.opticsexpress.org/abstract.cfm?URI=OPEX-7-2-77>
3. L. Novotny, M.R. Beversluis, K.S. Youngworth, and T.G. Brown, "Longitudinal field modes probed by single molecules," *Phys. Rev. Lett.* **86**, 5251–5254 (2001).
4. C.J.R. Sheppard and A. Choudhury, "Annular pupils, radial polarization, and superresolution," *Appl. Opt.* **43**, 4322–4327 (2004).
5. Q. Zhan, "Trapping metallic Rayleigh particles with radial polarization," *Opt. Express* **12**, 3377–3382 (2004),
<http://www.opticsexpress.org/abstract.cfm?URI=OPEX-12-15-3377>
6. S. Quabis, R. Dorn, M. Eberler, O. Glöckl and G. Leuchs, "Focusing light to a tighter spot," *Opt. Commun.* **179**, 1–7 (2000).
7. S. Quabis, R. Dorn, M. Eberler, O. Glöckl and G. Leuchs, "The focus of light – theoretical calculation and experimental tomographic reconstruction," *Appl. Phys. B* **72**, 109–113 (2001).
8. R. Dorn, S. Quabis and G. Leuchs, "Sharper focus for a radially polarized light beam," *Phys. Rev. Lett.* **91**, 233901 (2003).
9. J.T. Foley and E. Wolf, "Wave-front spacing in the focal region of high-numerical-aperture systems," *Opt. Lett.* **30**, 1312–1314 (2005).
10. T.D. Visser and J.T. Foley, "On the wavefront spacing of focused, radially polarized beams," *J. Opt. Soc. Am. A* **22**, 2527–2531 (2005).
11. D.W. Diehl and T.D. Visser, "Phase singularities of the longitudinal field components in the focal region of a high-aperture optical system," *J. Opt. Soc. Am. A* **21**, 2103–2108 (2004).
12. B. Richards and E. Wolf, "Electromagnetic diffraction in optical systems II. Structure of the image field in an aplanatic system," *Proc. Royal Soc. A* **253**, 358–379 (1959).

13. M. Born and E. Wolf, *Principles of Optics: Electromagnetic Theory of Propagation, Interference and Diffraction of Light*, seventh (expanded) ed. (Cambridge University Press, Cambridge, 1999). See especially Sec. 4.5.1.
14. J.F. Nye, *Natural Focusing and Fine Structure of Light* (Institute of Physics Publishing, Bristol, 1999). See especially Chapter 12.
15. G.P. Karman, A. van Duijl and J.P. Woerdman, "Unfolding of an unstable singularity point into a ring," *Opt. Lett.* **23**, 403–405 (1998).

1. Introduction

Recently, much research has been devoted to the focusing of radially polarized beams [1],[2]. Possible applications range from single molecule imaging [3, 4] to the trapping of metallic particles [5]. Radially polarized beams differ significantly from linearly polarized beams. For example, they can be focused to a narrower spot [6]–[8], with a field distribution that remains rotationally symmetric. Also, the field in the focal region has a stronger longitudinal component. Finally, the recently discovered irregularities in the wavefront-spacing in the focal region [9] are more pronounced for radially polarized fields than they are for linearly polarized fields [10].

The electric field in the focal region of a radially polarized beam has two non-zero parts, namely a radial component and a longitudinal component. In the present paper we examine the dependence of the electric energy density contributions of these two components on the angular aperture angle of the focusing system. Also, the behavior of the electric polarization ellipse in the focal plane is studied in detail. Finally, we demonstrate that the different components of the electric field possess phase singularities. Two different mechanisms for the creation or annihilation of these singularities are examined.

2. Focused, radially polarized fields

Consider an aplanatic focusing system L , as depicted in Fig. 1. The system has a focal length

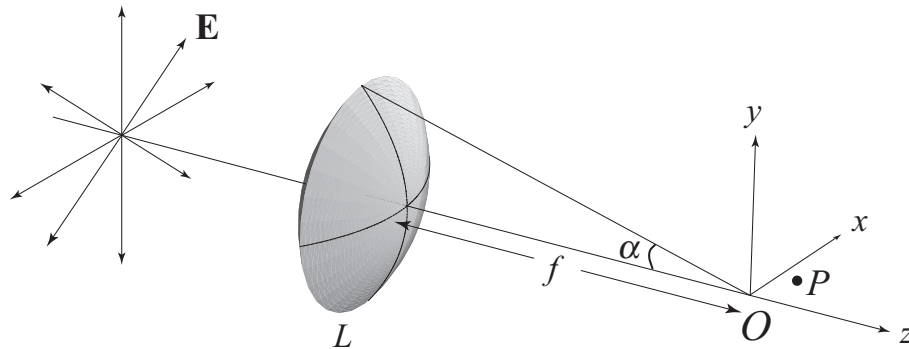


Fig. 1. Illustration of a high numerical aperture focusing system. The radially polarized incident beam propagates along the z -axis.

f and a semi-aperture angle α . The origin O of a right-handed cartesian coordinate system is taken to be at the geometrical focus. A monochromatic, radially polarized beam of frequency ω is incident on the system. The electric and magnetic fields at time t at position \mathbf{r} are given by the expressions

$$\mathbf{E}(\mathbf{r}, t) = \text{Re} [\mathbf{e}(\mathbf{r}) \exp(-i\omega t)], \quad (1)$$

$$\mathbf{H}(\mathbf{r}, t) = \text{Re} [\mathbf{h}(\mathbf{r}) \exp(-i\omega t)], \quad (2)$$

respectively, where Re denotes the real part. There are many ways to create a radially polarized beam (see, for example, Refs. [1] and [2] and the references therein). One of them is to combine

two, mutually orthogonally polarized, Hermite-Gaussian beams [3]. The longitudinal and radial components of the electric field at a point $P = (\rho_P, z_P)$ in the focal region are then given by the formulae [10]

$$e_z(\rho_P, z_P) = -ikf \int_0^\alpha l(\theta) \sin^2 \theta \cos^{1/2} \theta \times \exp(ikz_P \cos \theta) J_0(k\rho_P \sin \theta) d\theta, \quad (3)$$

$$e_\rho(\rho_P, z_P) = -kf \int_0^\alpha l(\theta) \sin \theta \cos^{3/2} \theta \times \exp(ikz_P \cos \theta) J_1(k\rho_P \sin \theta) d\theta, \quad (4)$$

where J_i is the Bessel function of the first kind of order i . Also, $l(\theta)$ denotes the *angular amplitude function*

$$l(\theta) = f \sin \theta \exp[-f^2 \sin^2 \theta / w_0^2], \quad (5)$$

where w_0 is the spot size of the beam in the waist plane, which is assumed to coincide with the entrance plane of the focusing system. On using the dimensionless *optical coordinates*

$$u = kz_P \sin^2 \alpha, \quad (6)$$

$$v = k\rho_P \sin \alpha, \quad (7)$$

Eqs. (3) and (4) can be rewritten as

$$e_z(u, v) = -ikf^2 \int_0^\alpha \sin^3 \theta \cos^{1/2} \theta \exp(-\beta^2 \sin^2 \theta) \times \exp(iu \cos \theta / \sin^2 \alpha) J_0\left(\frac{v \sin \theta}{\sin \alpha}\right) d\theta, \quad (8)$$

$$e_\rho(u, v) = -kf^2 \int_0^\alpha \sin^2 \theta \cos^{3/2} \theta \exp(-\beta^2 \sin^2 \theta) \times \exp(iu \cos \theta / \sin^2 \alpha) J_1\left(\frac{v \sin \theta}{\sin \alpha}\right) d\theta, \quad (9)$$

where the parameter $\beta = f/w_0$ denotes the ratio of the focal length of the system and the spot size of the beam in the waist plane. It follows from Eqs. (8) and (9) that the field has the following symmetry properties:

$$e_z(-u, v) = -e_z^*(u, v), \quad (10)$$

$$e_\rho(-u, v) = e_\rho^*(u, v), \quad (11)$$

where the asterisk denotes complex conjugation. It is seen from Eqs. (10) and (11) that, in addition to the rotational symmetry of the field components, the *time-averaged electric energy density* $w_e = \epsilon_0 \mathbf{E}^2(u, v)/2$ is symmetric about the focal plane. This quantity will be further investigated in the next Section.

3. The electric energy density

The time-averaged electric energy density consists of the sum of two contributions, viz.

$$w_e = \frac{\epsilon_0}{2} \mathbf{E}^2(u, v) = \frac{\epsilon_0}{4} \left[|e_\rho(u, v)|^2 + |e_z(u, v)|^2 \right], \quad (12)$$

where ϵ_0 denotes the permittivity in vacuum. One expects the relative contribution of the longitudinal field component to increase when the semi-aperture angle α increases. It is found that this is indeed the case. In Fig. 2 contours of the time-averaged electric energy densities $|e_\rho(u, v)|^2$ and $|e_z(u, v)|^2$ are shown, both normalized to the same value. In this example $\alpha = \pi/6$, and it is seen that the contribution of the radial field component dominates at most points. The reverse is true, however, for larger values of α . This is illustrated in Fig. 3 in which

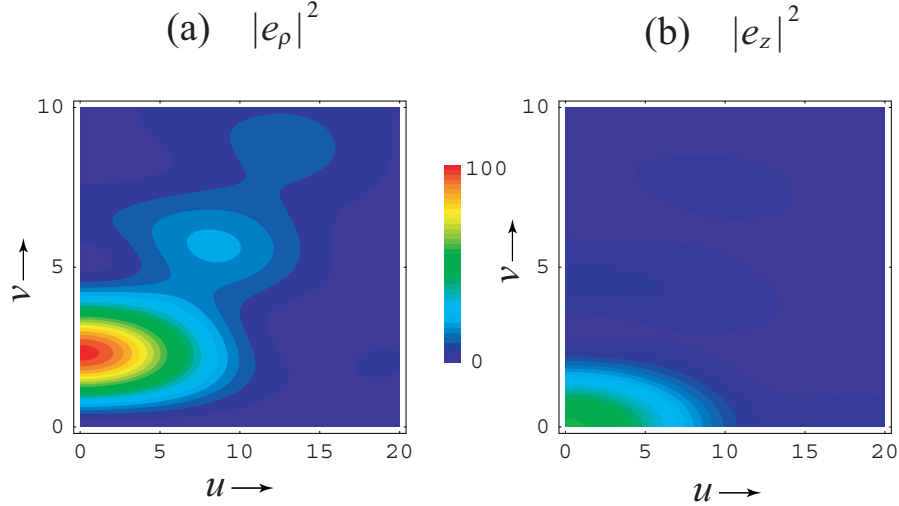


Fig. 2. Contours of $|e_\rho(u, v)|^2$ (a) and $|e_z(u, v)|^2$ (b). In this example the semi-aperture angle $\alpha = \pi/6$, and the beam parameter $\beta = 0.6$.

contours for the same two energy density contributions are shown for the case that the semi-aperture angle $\alpha = \pi/3$. Now the contribution of the longitudinal field component is clearly dominant at most points in the focal region. These results are in agreement with earlier observations [2, 3].

4. The state of polarization in the focal plane

It is seen from Eqs. (8) and (9) that in the focal plane ($u = 0$) the longitudinal electric field component $e_z(0, v)$ is purely imaginary, whereas the radial electric field component $e_\rho(0, v)$ is real-valued. Thus, for all points in the focal plane we can separate the real and imaginary part of the electric field and write

$$\mathbf{e}(0, v) = e_\rho(0, v)\hat{\boldsymbol{\rho}} + i\text{Im}[e_z(0, v)]\hat{\mathbf{z}}, \quad (13)$$

with $\hat{\boldsymbol{\rho}}$ and $\hat{\mathbf{z}}$ unit vectors in the radial and the longitudinal direction, respectively, and Im denotes the imaginary part. Since $e_\rho(0, v)\hat{\boldsymbol{\rho}}$ and $e_z(0, v)\hat{\mathbf{z}}$ are perpendicular to each other, they constitute the conjugate semi-axes of the polarization ellipse. Moreover, $\hat{\boldsymbol{\rho}}$ lies in the focal plane, whereas $\hat{\mathbf{z}}$ is perpendicular to it. Hence, *the polarization ellipse of the electric field at any point in the focal plane is at right angles to the focal plane*. Also, the plane of polarization (i.e., the plane formed by the polarization ellipse) at a point $(x, y, 0) = (v \cos \phi, v \sin \phi, 0)$ makes an angle ϕ with the xz -plane. The two axes of the polarization ellipse are in the ratio

$$R(v) = \frac{|\text{Im}[e_z(0, v)]|}{|e_\rho(0, v)|}. \quad (14)$$

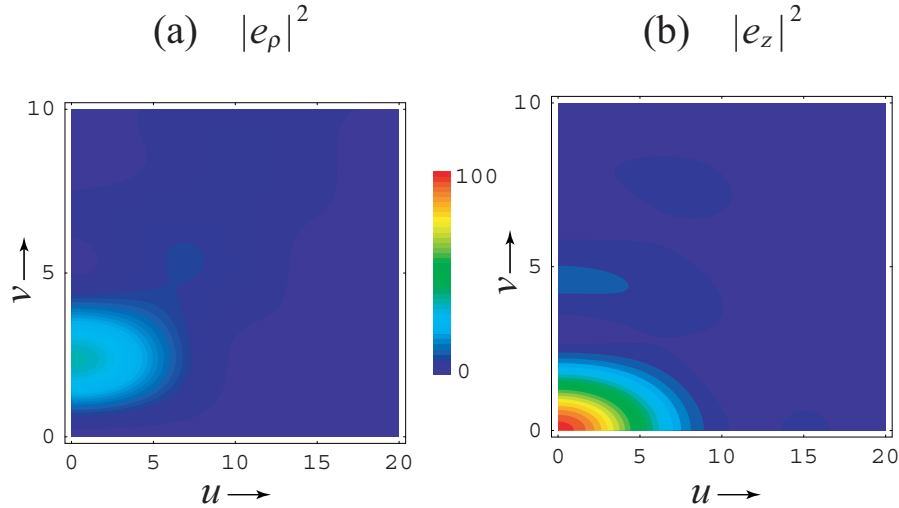


Fig. 3. Contours of $|e_\rho(u, v)|^2$ (a) and $|e_z(u, v)|^2$ (b). In this example the semi-aperture angle $\alpha = \pi/3$, and the beam parameter $\beta = 0.6$.

The behavior of the two normalized electric field components $e_\rho(0, v)/\text{Im}[e_z(0, 0)]$ and $\text{Im}[e_z(0, v)]/\text{Im}[e_z(0, 0)]$ and the ratio $R(v)$ are both shown in Fig. 4. It is seen that at certain circles in the focal plane (e.g., $v = 3.0, 6.7$) the electric field is purely radial, whereas at others (e.g., $v = 0, 5.2$) the electric field is purely longitudinal. At the former points the field is linearly polarized along the radial direction with the ratio R being zero; at the latter points the field is linearly polarized along the z -direction with R being infinite. Both sets of circles constitute so-called *L-lines* in the focal plane [14]. We note that at points such as $v = 1.4, 4.4, 5.9$ where $R(v)$ equals unity (indicated by the dashed line in Fig. 4b), the polarization is circular. In other words, the circles $v = 1.4, 4.4, 5.9$ form so-called *C-lines* in the focal plane.

The sense in which the electric polarization ellipse is traversed (i.e., its 'handedness') can be determined by noting from Eqs. (1) and (13) that $\mathbf{E}(0, v, t = 0) = e_\rho(0, v)\hat{\rho}$, whereas a quarter period later one has $\mathbf{E}(0, v, t = \pi/2\omega) = \text{Im}[e_z(0, v)]\hat{z}$. This implies that if, on varying the radial distance v , one of the two electric field components changes sign, then so does the handedness of the state of polarization. Stated differently, *in the focal plane the L-lines (at which the polarization is linear) separate rings in which the electric polarization ellipse is being traversed in opposite directions*. The electric polarization ellipse and its handedness are shown in Fig. 5 for selected values of the radial position v . As a side remark we note, as can be seen from Fig. 4(a), that everywhere in the focal plane at least one of the two electric field components is non-zero. Hence, in contrast to focused linearly polarized fields [12], nowhere in the focal plane does the total electric energy density (given by Eq. (12)) vanish.

5. Phase singularities

In a previous paper we showed that the longitudinal electric field component of strongly focused, linearly polarized beams exhibits phase singularities [11]. We also showed that these singularities can be created or annihilated when the semi-aperture angle of the focusing system is changed. We now examine the existence of phase singularities of the two field components of the electric field in the focal region of focused, radially polarized beams. The presence of singular points (i.e., points of zero amplitude) of both e_z and e_ρ in the focal plane is evident

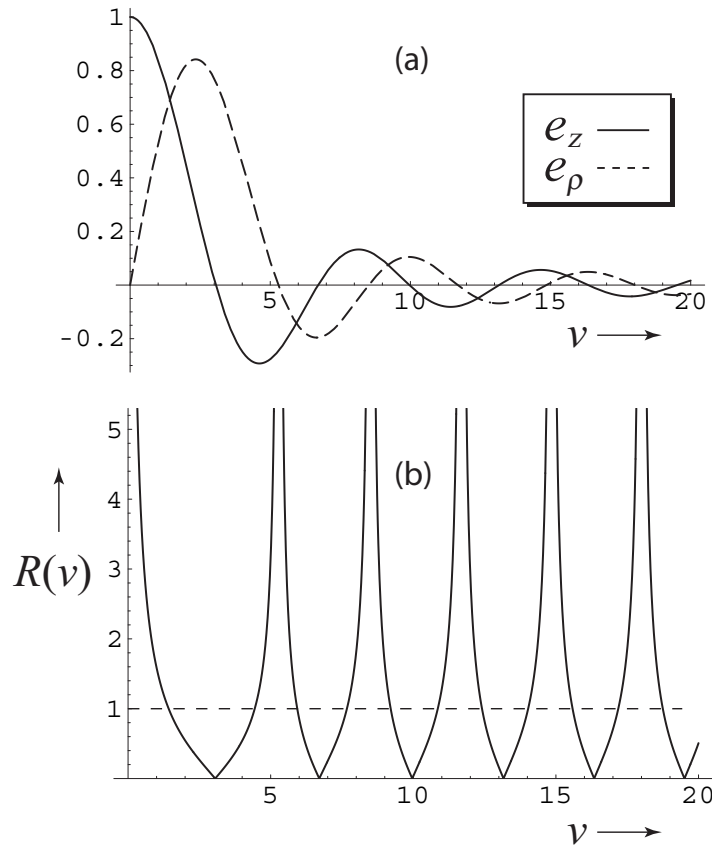


Fig. 4. (a) Plot of the normalized electric field components $e_\rho(0, \nu)/\text{Im}[e_z(0, 0)]$ (dashed curve) and $\text{Im}[e_z(0, \nu)]/\text{Im}[e_z(0, 0)]$ (solid curve). (b) Plot of $R(\nu)$, the ratio of the lengths of the two conjugate semi-axes of the electric polarization ellipse. The different intersections with the horizontal dashed line (at which $R(\nu) = 1$) are points at which the polarization is circular. In this example the semi-aperture angle $\alpha = \pi/4$, and the beam parameter $\beta = 0.6$.

from the zero-crossings of the field components depicted in Fig. 4(a). Additional singularities of e_z are seen in Figs. 6 and 7 in which the phase of the field component is indicated by color. At points where different colors meet the field amplitude is zero and, consequently, the phase of the field component is singular.

In the description of linearly polarized light there is only a single free parameter, namely the semi-aperture angle α [11]. However, in the model for radially polarized light, there is an additional free parameter, the beam parameter β (See Eqs. (8) and (9)). One might therefore guess that there are two different mechanisms for the creation or annihilation of phase singularities, namely varying the semi-aperture angle α , and varying the beam parameter β . This is found to be indeed the case. In Figure/Movie 6 an example of annihilations of phase singularities of the longitudinal field component e_z caused by smoothly increasing the semi-aperture angle α is presented. For, for example, $\alpha \approx 51.7^\circ$ an annihilation event can be seen near $(u, \nu) = (22, 10)$.

In Figure/Movie 7, the behavior of the same field component for varying values of the beam parameter β is shown. Again, several annihilation events can be observed.

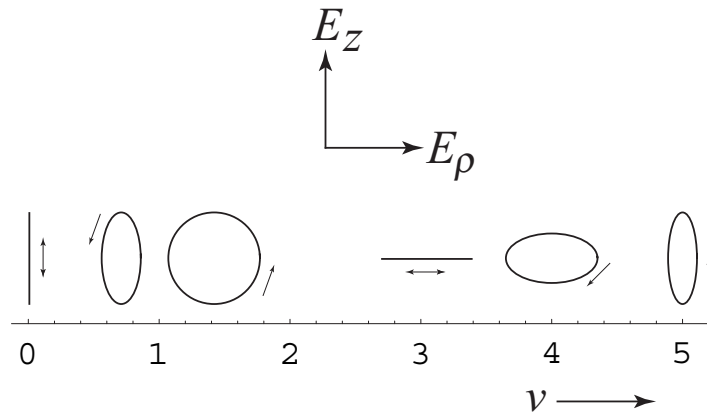


Fig. 5. The electric polarization ellipse in the focal plane for selected values of the radial distance ($v = 0.00, 0.71, 1.42, 3.05, 4.00, 5.00$). The arrow indicates the direction in which the ellipse is being traversed. In this example the semi-aperture angle $\alpha = \pi/4$, and the beam parameter $\beta = 0.6$.

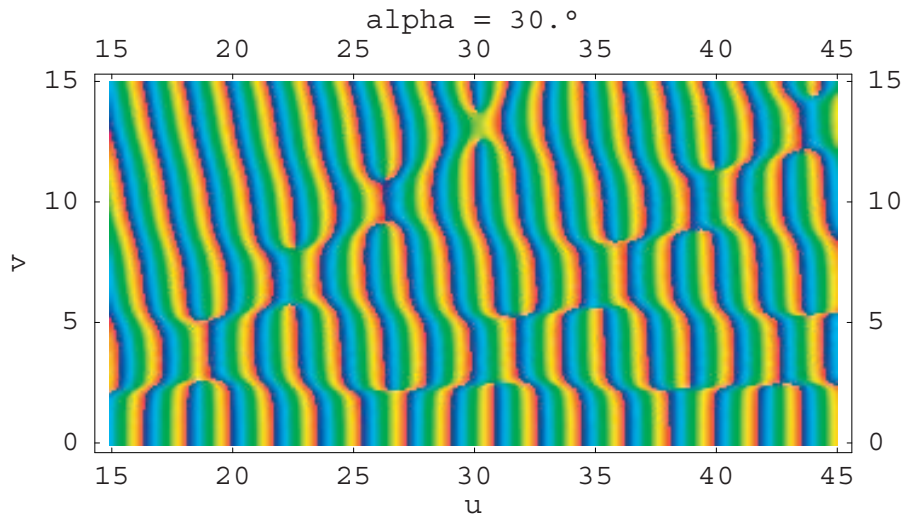


Fig. 6. Color-coded plot of the phase of the longitudinal electric field component e_z for different values of the semi-aperture angle α . In this example $\beta = 0.6$.

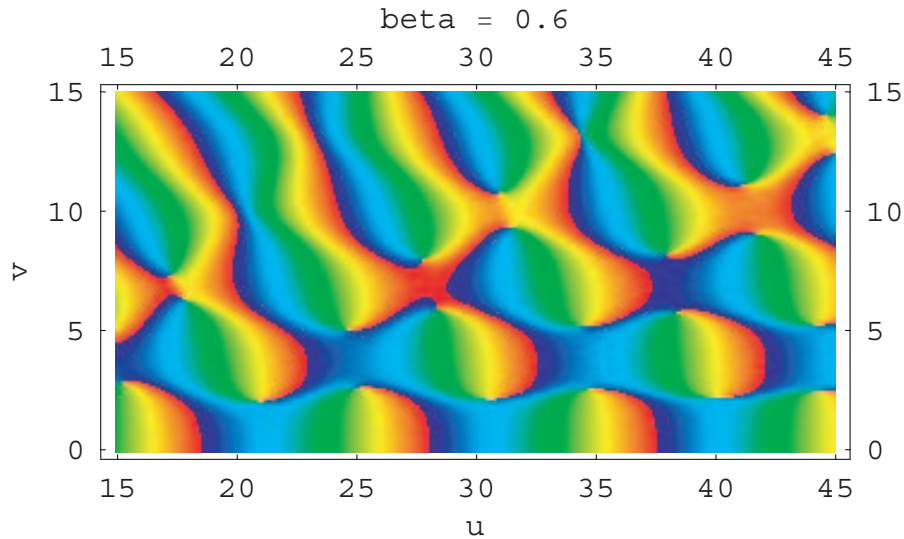


Fig. 7. Color-coded plot of the phase of the longitudinal electric field component e_z for different values of the beam-size parameter β . In this example $\alpha = \pi/3$.

As mentioned above, the radial field component e_ρ also possesses phase singularities. In Figure/Movie 8 it is shown how an Airy ring-like singularity is created on the z -axis when the beam parameter β is varied. This is reminiscent of an experimental observation reported in [15].

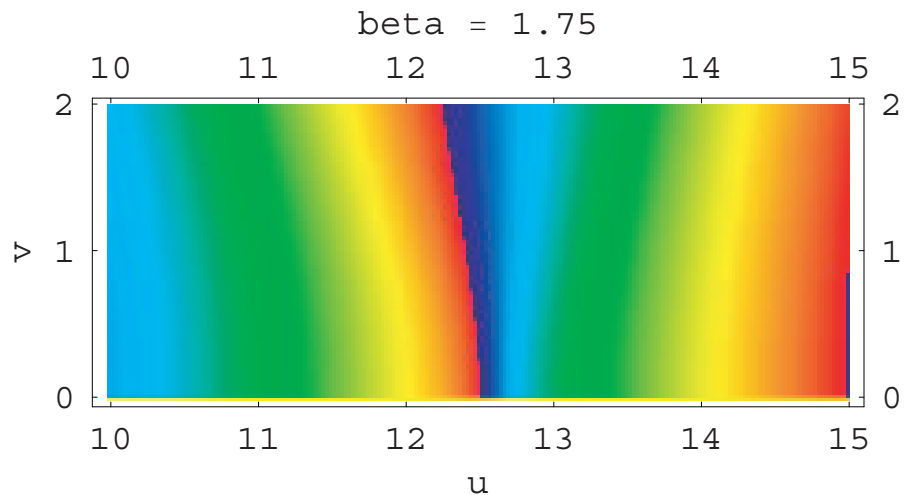


Fig. 8. Color-coded plot of the phase of the radial electric field component e_ρ for different values of the beam-size parameter β . When β is decreased, an Airy ring-like singularity is created. In this example $\alpha = \pi/4$.

6. Conclusions

We have examined the structure of strongly focused, radially polarized fields. It was found that the relative contribution to the time-averaged electric energy density of the longitudinal field

component increases with increasing semi-aperture angle.

It was shown that in the focal plane there are circular L -lines at which the electric polarization is linear. These S -lines separate rings in which the electric polarization has an opposite handedness.

The existence of phase singularities of both components of the electric field was demonstrated. There are two different ways in which these singularities may be created or annihilated, namely by variation of the semi-aperture angle, or by variation of the beam size parameter.

Acknowledgments

R.W.S. wishes to thank the Fulbright Center for their financial support.